

Supplementary Information

(Dated: August 5, 2007)

I. SAMPLE QUALITY AND REPRODUCIBILITY OF THE GAP

We have measured samples prepared in two ways, prepared *in situ* and annealed after exposure to air. We observed a similar gap in both cases. The EDC near E_F shows half width half maximum of only 30 meV, suggesting that the sample is of extremely high quality. We also note that the background intensity in the single layer graphene sample is extremely weak (less than 1% of the main peak), which is another indication of high sample quality.

II. SAMPLE THICKNESS

We have measured the dispersion in single layer graphene as a function of k_x and k_z in two k_z Brillouin zones (Fig.S1) and no k_z dispersion is observed, in agreement with reported results for single layer graphene [1]. The lack of splitting in the π band dispersion (Fig.1a) is also in support of the 1ML thickness of the single layer sample.

III. ACCURATE DETERMINATION OF THE K POINT

We aligned the sample first by taking the data near the two K points (Fig.S2). From the symmetry, we determined the Γ point to be accurate within $\pm 0.25^\circ$ and azimuthal angle to be accurate within 0.2° . Then we took many angles near the one K point with a fine step of 0.05° , which converts to a step of 0.003 \AA^{-1} in k for 50 eV photon energy. Figure S3 shows data taken near the K point with small step. We note that the dipole matrix element for graphene strongly depends on the Brillouin zone, similar to the case of graphite [2]. As is shown in Fig.S3(h,i), above E_D (panel h), the intensity is enhanced outside the first Brillouin zone, while below E_D , the intensity is enhanced inside the first Brillouin zone. This strong dependence of intensity on its momentum space (i.e. whether it is inside or outside the Brillouin zone) can be used for accurate determination of the K point. Fig.S3(g) shows the EDCs at $k_y=0$ for data shown in Figs.S3(a-f). From the relative peak intensity, the K point is determined to be at the angle of panel c, where the two EDC peaks at the K point have almost equal intensity. In this way, the K point is determined to be accurate within 0.003 \AA^{-1} . Fig.S3(h) shows the gap as a function of k_x , where a minimum gap of 0.26 eV is observed at the K point. This accurate determination of the K point shows that the gap is intrinsic to the data at the K point, not an artifact due to deviation from the K point.

We would like to point out that the geometry used in this manuscript is the best geometry to extract information on both the conical dispersion and the presence of a gap. This geometry in fact allows to measure both sides of the cones and to distinguish the top and bottom of the bands. Also the use of this geometry is important as it allows to resolve two peaks in the EDC if presents.

IV. BLOCH HAMILTONIANS FOR SINGLE AND BILAYER GRAPHENE

For single layer graphene, the Bloch Hamiltonian associated with wave vector \mathbf{k} is given by

$$h(\mathbf{k}, m) = \begin{pmatrix} m & t_1 S_1(\mathbf{k}) \\ t_1 S_1^*(\mathbf{k}) & -m \end{pmatrix}. \quad (1)$$

Here t_1 is the nearest neighbor hopping matrix element, $2m$ is the difference between the substrate potential on the A and B sublattices and $S_1(\mathbf{k}) = (1 + e^{-i\mathbf{k}\cdot\mathbf{a}} + e^{-i\mathbf{k}\cdot\mathbf{a}+i\mathbf{k}\cdot\mathbf{b}})$, where \mathbf{a} and \mathbf{b} are the unit vectors. The wave vector associated with the Dirac point \mathbf{k}_D satisfies $S_1(\mathbf{k}_D) = 0$. Clearly there is a gap $\Delta=2m$ between the two eigenenergies when $m \neq 0$.

For bilayer graphene, the Bloch Hamiltonian is given by

$$H(\mathbf{k}) = \begin{pmatrix} h(\mathbf{k}, m_1) & v(\mathbf{k}) \\ v^\dagger(\mathbf{k}) & h(\mathbf{k}, m_2) \end{pmatrix}. \quad (2)$$

Here m_1 and m_2 are the sublattice symmetry breaking parameters in the bottom (buffer layer) and top graphene layer, and

$$v(\mathbf{k}) = \begin{pmatrix} 0 & t_\perp e^{i\mathbf{k}\cdot(\mathbf{b}-\mathbf{a})} \\ t'_\perp (1 + e^{i\mathbf{k}\cdot\mathbf{a}} + e^{i\mathbf{k}\cdot\mathbf{b}}) & t'_\perp (1 + e^{i\mathbf{k}\cdot\mathbf{b}} + e^{i\mathbf{k}\cdot(\mathbf{b}-\mathbf{a})}) \end{pmatrix}, \quad (3)$$

where t_\perp and t'_\perp are the interlayer hopping parameters.

V. BREAKING OF THE SIX FOLD SYMMETRY

To take into account the effect of scattering due to the substrate $6\sqrt{3}\times 6\sqrt{3}\text{R}30^\circ$ potential, we couple each \mathbf{k} point with six others according to the following Hamiltonian

$$\mathcal{H}(\mathbf{k}) = \begin{pmatrix} d & u_1 & u_2 & u_3 & u_4 & u_5 & u_6 \\ u_1^\dagger & d_1 & 0 & 0 & 0 & 0 & 0 \\ u_2^\dagger & 0 & d_2 & 0 & 0 & 0 & 0 \\ u_3^\dagger & 0 & 0 & d_3 & 0 & 0 & 0 \\ u_4^\dagger & 0 & 0 & 0 & d_4 & 0 & 0 \\ u_5^\dagger & 0 & 0 & 0 & 0 & d_5 & 0 \\ u_6^\dagger & 0 & 0 & 0 & 0 & 0 & d_6 \end{pmatrix}. \quad (4)$$

Here $d = h(\mathbf{k}, m)$ is the 2×2 matrix given in Eq. (1), and $d_i = h(\mathbf{k} + \mathbf{G}_i, m)$ where

$$\begin{aligned} \mathbf{G}_1 &= s\left(\frac{2\pi}{3\sqrt{3}}, \frac{2\pi}{3}\right), & \mathbf{G}_2 &= s\left(\frac{4\pi}{3\sqrt{3}}, 0\right) \\ \mathbf{G}_3 &= s\left(\frac{2\pi}{3\sqrt{3}}, -\frac{2\pi}{3}\right), & \mathbf{G}_4 &= s\left(-\frac{2\pi}{3\sqrt{3}}, -\frac{2\pi}{3}\right) \\ \mathbf{G}_5 &= s\left(-\frac{4\pi}{3\sqrt{3}}, 0\right), & \mathbf{G}_6 &= s\left(-\frac{2\pi}{3\sqrt{3}}, \frac{2\pi}{3}\right) \end{aligned} \quad (5)$$

are the second shortest reciprocal lattice vectors of the $6\sqrt{3}\times 6\sqrt{3}\text{R}30^\circ$ superstructure with $s = \frac{3}{13}$. In Eq. (4), $u_i = g_i \begin{pmatrix} 1 & 0 \\ 0 & 1 \end{pmatrix}$. In the presence of 6-fold rotational symmetry, all the g_i 's should be the same. When the 6-fold rotational symmetry is broken down to 3-fold, the six g_i 's are divided into two groups (each containing three g_i 's) with different values. Fig.4e is obtained for a particular choice of the two g values (0.75 and 0).

-
- [1] Ohta, T., Bostwick, A., Seyller, T., Horn, K., Rotenberg, E. Controlling the electronic structure of bilayer graphene. *Science* **313**, 951 (2006).
- [2] Shirley, Eric L., Terminello, L.J., Santoni, A. and Himpsel, F.J. Brillouin-zone-selection effects in graphite photoelectron angular distributions. *Phys. Rev. B* **51**, 013614 (1995).

FIG. 1: ARPES intensity map taken near the K point on single layer graphene as a function of k_{\parallel} and k_z at -1 eV. The data are normalized to have the sample peak amplitude. The absence of k_z dispersion confirms that this sample is single layer graphene.

FIG. 2: (a) Intensity map taken as a function of theta and tilt angles at -0.4 eV at 50 eV photon energy. The black lines show the intensity at tilt=0. From the peak positions, Γ and K points are determined to be accurate within 0.25° . (b) Intensity as a function of tilt angle taken at the positions of the blue and red broken lines indicated in panel a. From the separation of the peak positions, the azimuth angle is determined to be accurate within 0.2° .

FIG. 3: (a-f) ARPES intensity maps taken on single layer graphene as a function of energy and momentum for accurate determination of the K point. The positions for these cuts are indicated by the lines in the panels h and i. The dotted curves in each panel are the dispersions extracted from EDCs. The gray horizontal lines mark the minimum gap region defined by the cut through the K point (panel c). The inset between panels a and b show a schematic drawing for the conical dispersion and a cut away from the K point, where a gap is expected. (g) Energy distribution curves at $k_y=0$ for data shown in panels a-f. (h) Gap as a function of k_x , which shows a minimum of 0.26 eV at the K point. (i, j) Intensity maps as a function of k_x and k_y at E_F and -1.0 eV respectively. Because of the dipole matrix element [2], the intensity above E_D (panel h) is enhanced outside the first Brillouin zone while below E_D (panel i), the intensity is enhanced inside the first Brillouin zone.

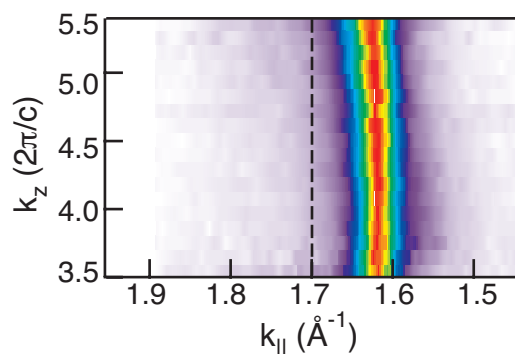


Fig S1

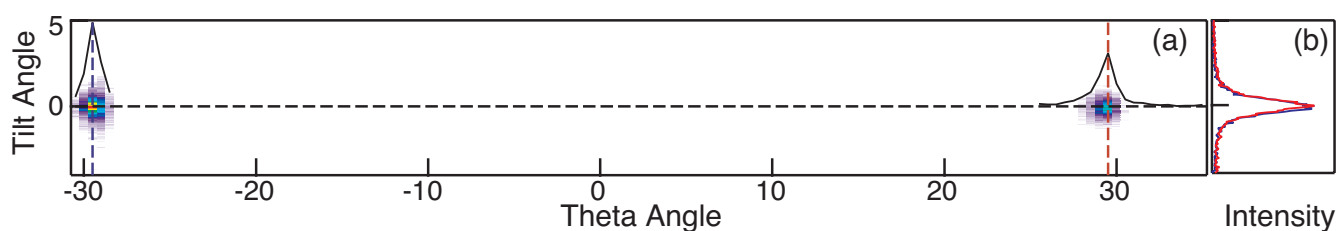


Fig S2

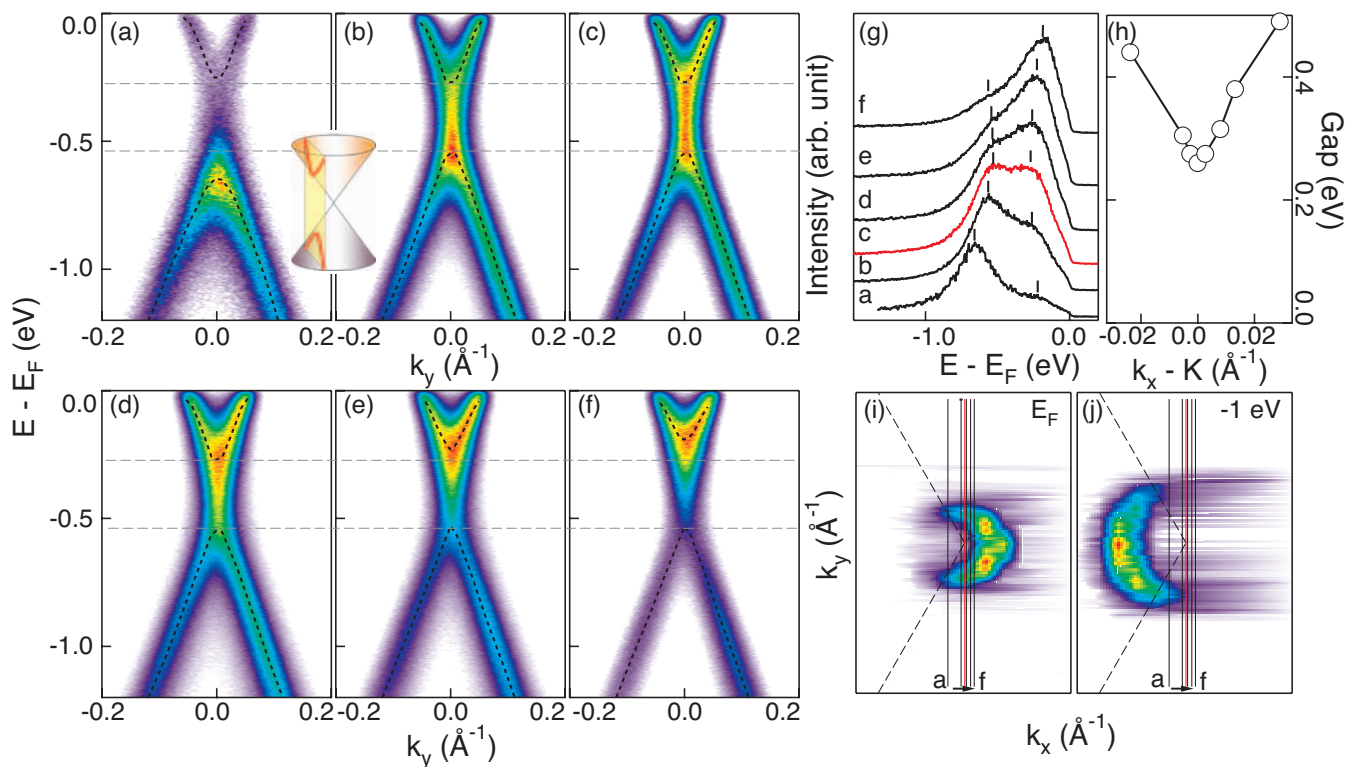


Fig S3